VIP Molecular Switches Very Important Paper

DOI: 10.1002/anie.201402294

# A Rapidly Reversible Chemical Dimerizer System to Study Lipid Signaling in Living Cells**

*Suihan Feng, Vibor Laketa, Frank Stein, Anna Rutkowska, Aidan MacNamara, Sofia Depner, Ursula Klingmüller, Julio Saez-Rodriguez, and Carsten Schultz**

***Abstract:*** *Chemical dimerizers are powerful tools for non-invasive manipulation of enzyme activities in intact cells. Here we introduce the first rapidly reversible small-molecule-based dimerization system and demonstrate a sufficiently fast switch-off to determine kinetics of lipid metabolizing enzymes in living cells. We applied this new method to induce and stop phosphatidylinositol 3-kinase (PI3K) activity, allowing us to quantitatively measure the turnover of phosphatidylinositol 3,4,5-trisphosphate ($PIP_3$) and its downstream effectors by confocal fluorescence microscopy as well as standard biochemical methods.*

To artificially control intracellular enzymes and entire signaling networks, small-molecule inhibitors or several genetic techniques such as RNAi or overexpression are available. While these methods are very useful and well established, they are mostly not suitable for rapidly switching enzyme activities on and off inside cells. Apart from a few examples,[1] switching on enzymes on a multiple-second timescale is often performed by inducing protein dimerization with rapamycin.[2] The most commonly used strategy is the fast induced translocation of proteins to their sites of action, for example, from the cytosol to the plasma membrane, by forming the ternary FKBP–rapamycin–FRB complex (FKBP: FK506 binding protein; FRB: FKBP12-rapamycin binding domain). This may be conveniently followed by standard microscopy methods. Using this approach, a variety of signaling proteins, such as lipid phosphatases[3] and kinases[4] have been successfully activated in living cells. Recently, other natural-product-based chemical dimerizer systems such as gibberellin,[5] ABA,[6] or fusicoccin[7] have been developed to act orthogonally to the rapamycin system. In addition, newly emerging protein labeling techniques[8] provide another way of designing synthetic chemical dimerizers.[9] However, all mentioned chemical induced dimerization (CID) systems are generally irreversible, unless a sophisticated technique that requires two CID systems is applied,[10] or extensive washing steps are involved.[7] Recently, optically switchable systems based on the conformational changes of phytochromes[11] or LOV[12] domains were introduced to activate enzymes with minimal perturbation of the intact cell. The optogenetic strategy enables to perform the dimerization process in a reversible manner on the single cell level, which is especially convenient for fluorescent microscopy experiments. While these methods are capable of inducing dimerization within seconds, the reversing process generally takes several minutes. Only the technique developed by Weiner et al.[11a,d] allows stopping the dimerization process in around five seconds by another light source in the presence of an added co-factor. However, the dependence on the light sources implies that these methods are less convenient for following events by standard biochemical batch methods such as Western blots.[13]

Here, we introduce a novel reversible dimerization system based on a standard design (Figure 1a) that brings a given active enzyme to a defined cellular location by adding the reversible chemical dimerizer (rCD1, Figure 1b). In a second step, the translocated enzyme is rapidly removed by addition of a commercially available competing ligand (FK506). In our application, this permits to study the accumulation of a lipid product ($PIP_3$) and its subsequent metabolism at the single cell level by fluorescence microscopy. In addition, this method is compatible with conventional biochemistry tools to study signaling patterns such as protein phosphorylation levels on a batch scale.

Aiming to produce a generic system, our dimerization approach is based on two standard protein fusions, FKBP[8a] and the SNAP-tag (Figure 1a).[8b] The latter has been extensively used for intracellular protein labeling in intact cells. While the SNAP-tag covalently reacts with molecules featuring a benzylguanine moiety, the FKBP protein binds a number of ligands with nanomolar affinity. A large number of FKBP and SNAP-tag fusion proteins are already available from earlier studies[2] and may be directly used with rCD1 in the future. To obtain rCD1 (Figure 1b), we synthetically connected a benzylguanine moiety via a short linker to SLF (synthetic ligand of FKBP) in good yield (48% in two steps, Scheme S1 in the Supporting Information).

[*] S. Feng, Dr. V. Laketa, F. Stein, Dr. A. Rutkowska, Priv.-Doz. Dr. C. Schultz
Cell Biology & Biophysics Unit
European Molecular Biology Laboratory
Meyerhofstrasse 1, 69117 Heidelberg (Germany)
E-mail: schultz@embl.de
Dr. A. MacNamara, Dr. J. Saez-Rodriguez
European Molecular Biology Laboratory, European Bioinformatics Institute (EBI), Wellcome Trust Genome Campus, Hinxton, Cambridge CB10 1SD (UK)
Dr. S. Depner, Prof. U. Klingmüller
Systems Biology of Signal Transduction
German Cancer Research Center (DKFZ)
Im Neuenheimer Feld 280, 29121 Heidelberg (Germany)

[**] This work was supported by the DFG (Transregio 83). We are grateful for expert support of EMBL's Advanced Light Microscopy Facility (ALMF) and to Dr. André Nadler for critical reading of the manuscript.

Supporting information for this article is available on the WWW under http://dx.doi.org/10.1002/anie.201402294.

  

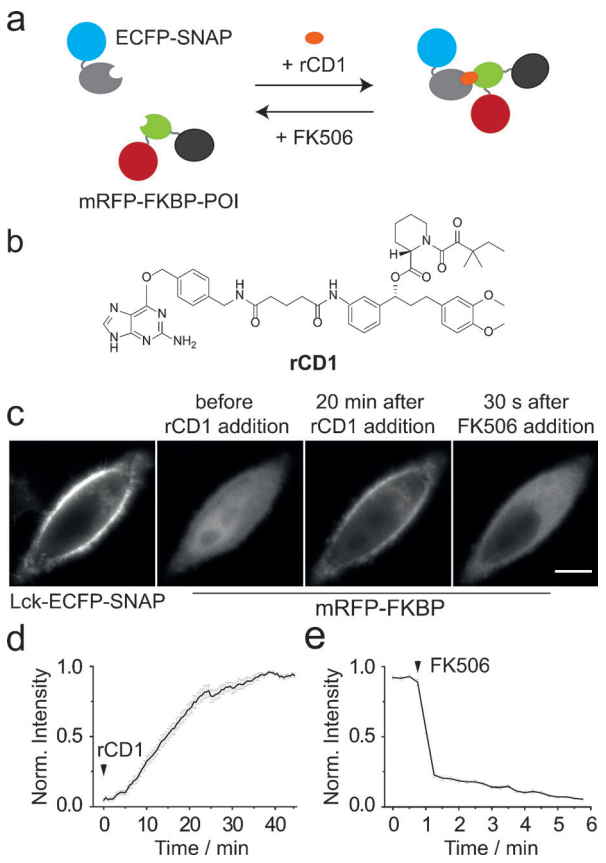


***Figure 1.*** a) rCD1-Based dimerization system. b) Chemical structure of rCD1 (see synthetic details in Supporting Information). c) Representative time-lapse fluorescence images of HeLa cells co-transfected with Lck-ECFP-SNAP$_f$ and mRFP-FKBP constructs. rCD1 (1 μM) induced translocation of mRFP-FKBP to the plasma membrane and release of mRFP-FKBP after addition of FK506 (1 μM). Scale bar indicates 10 μm. d,e) Quantification of translocation induced by rCD1 (d) and reverse translocation upon FK506 addition (e). rCD1 and FK506 were added as indicated by black arrows. The normalized intensity (*Y*-axis) was derived by using the "Protein Translocation Quantification Macro" (details see Supporting Information). Error bar represents the standard error of the mean from at least three independent experiments ($n > 10$).

We expressed the plasma membrane-associated Lck-ECFP-SNAP$_f$ tag and the mRFP-FKBP fusion protein in HeLa Kyoto cells. While the SNAP-tag fusion resided at the plasma membrane, the latter construct was evenly distributed in the cytoplasm and nucleus (Figure 1c). Addition of rCD1 induced translocation of the red fluorescent protein to the plasma membrane within 30 min (Figure 1d) with a detectable onset after 5 min (Movie S1), thus demonstrating rCD1-induced protein dimerization in living cells. As the onset of the translocation was comparably slow, we microinjected rCD1 into cells just after treatment with the compound extracellularly (data not shown). However, this preliminary experiment did not speed up translocation of mRFP-FKBP suggesting that the SNAP-tag labeling reaction and not cell entry was the time-limiting step. Subsequent addition of FK506, a compound that efficiently competes with SLF for the binding to FKBP, induced very fast release of mRFP-FKBP from the plasma membrane with a half-life of less than 15 s (Figure 1e, Movie S2). This rapid reversibility permitted us to estimate the kinetics of an rCD1-induced signal at the plasma membrane after eliminating the activator (see below). Since FK506 is known to inhibit calcineurin,[14] we performed a control experiment to check if the dimerization process competes with the rapamycin analogue AP23102 (a so-called rapalog), which is ineffective on calcineurin yet exhibits a similar affinity to FKBP.[15] As expected, the addition of AP23102 also led to fast release of mRFP-FKBP from the plasma membrane (Figure S1).

To determine whether rCD1 reversibly induces translocation to another cell compartment, we expressed NLS$_2$-SNAP$_f$-ECFP localized to the nucleus and the mRFP-FKBP construct in HeLa Kyoto cells. The latter translocated to the nucleus after addition of rCD1 within 60 min, and was released back to the cytoplasm within 10 min after adding FK506 (Figure S2). The slower kinetics is likely due to the stringent regulation of nuclear transport by nuclear pore complexes.

For an initial biological application, we investigated the induction of phosphatidylinositol 3-kinase (PI3K) activity in HeLa cells.[4] PI3K phosphorylates the common phosphoinositide PI(4,5)P$_2$ to the second messenger PI(3,4,5)P$_3$ (PIP$_3$) which is typically monitored by translocation of the pleckstrin homology domain of Akt (PH$_{Akt}$) fused to a fluorescent protein. Again, we expressed Lck-ECFP-SNAP$_f$ as a membrane anchor and an N-terminal fusion of the mRFP-FKBP construct with the inter-Src homology 2 (iSH2) domain from p85, which complexes in cells with the endogenous catalytic unit p110α of PI3K.[4] Translocation of the iSH2 domain was induced by adding rCD1 (1 μM) and the formation of PIP$_3$ was monitored by quantifying EGFP-PH$_{Akt}$ translocation to the plasma membrane (Figure 2a,b). Comparison of the onset kinetics of iSH2 and PH domain translocation (Figure 2c) suggested that small amounts of iSH2 domain at the plasma membrane are sufficient to activate the PI3K pathway. Similar experiments with the above design in HEK293T cells generated comparable PH$_{Akt}$ translocation patterns as well as typical membrane ruffling (Figure S3), an indicator of PIP$_3$ accumulation at the plasma membrane.[16] Subsequent addition of FK506 not only reversed binding of the iSH2 construct to the plasma membrane, but also resulted in an instantaneous release of the PH$_{Akt}$ to the cytosol (Figure 2c, Figure S4, Movie S3). As PH$_{Akt}$ detects both PI(3,4)P$_2$ and PI(3,4,5)P$_3$, this fast release is likely indicative of dephosphorylation to PI(4,5)P$_2$ by PTEN and less so of the 5-phosphatase SHIP.

As the PIP$_3$ disappearance was apparently driven by very fast enzymatic reactions, it was essential to understand whether the PI3K release was kinetically contributing to the PIP$_3$ decay or if the release of PH$_{Akt}$ predominantly represented PTEN activity. Therefore, we quantified the release of iSH2 and PH$_{Akt}$ constructs induced by increasing FK506 concentrations. By fitting single cell traces with monoexponential decay functions, we calculated the corresponding half-life times ($t_{1/2}$) of iSH2 domains and EGFP-PH$_{Akt}$ indicative of PI3K activity and its lipid products, respectively, for the entire titration series (Figure 2d). We observed a relatively stable $t_{1/2}$ value ($\approx$40 s) for PIP$_3$ breakdown for concentrations above

  

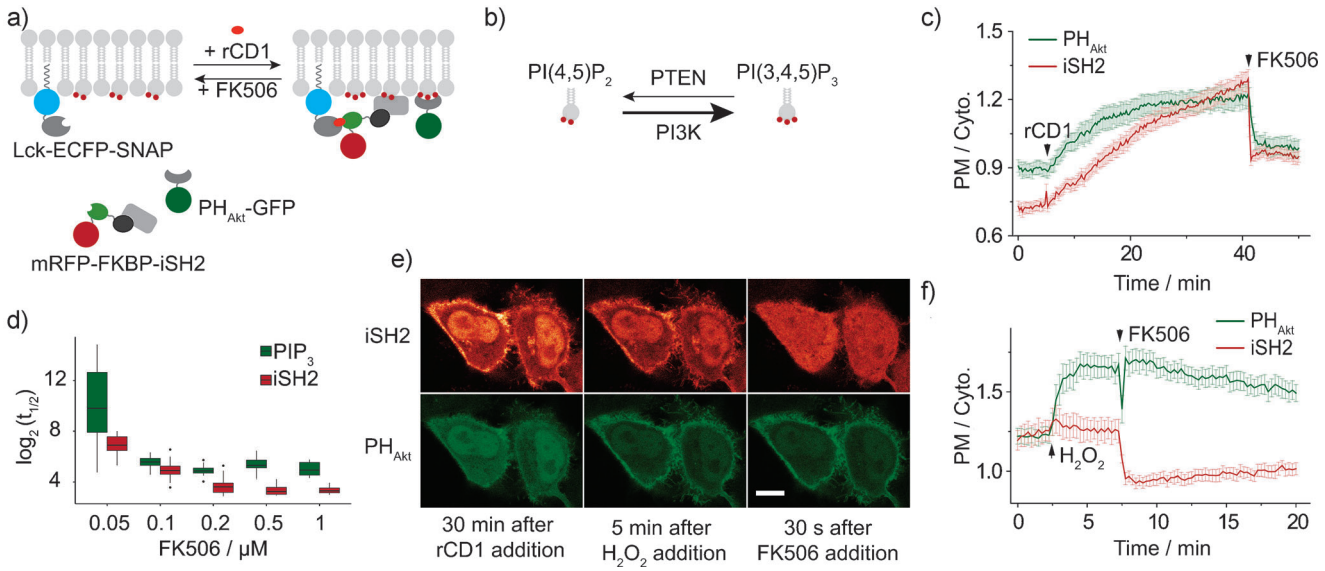


***Figure 2.*** a) PI3K activation induced by rCD1 and subsequent deactivation after FK506 addition. b) PI3K converts PI(4,5)$P_2$ to PI(3,4,5)$P_3$ which recruits the PH domain of Akt. At the same time, this process is down-regulated by PTEN. c) Quantification analysis of EGFP-PH$_{akt}$ and mRFP-FKBP-iSH2. rCD1 and FK506 were added as indicated by black arrows. The ratio of plasma membrane and cytosol (PM/Cyto) was calculated by analyzing the raw image data using the "Protein Translocation Quantification Macro" (details see Supporting Information). Error bar represents the standard error of the mean from at least three independent experiments ($n > 10$). d) Half-life ($t_{1/2}$) of $PIP_3$ (measured by EGFP-PH$_{Akt}$) and iSH2 translocation kinetics after addition of various amounts of FK506. e) Representative images of HeLa cells stimulated with $H_2O_2$ and FK506. Cells were pre-treated with rCD1 for 30 min before image recording. Note the quick release of the iSH2 complex and the persistence of the PH$_{Akt}$ at the plasma membrane after $H_2O_2$ addition. Scale bar indicates 10 µm. f) Quantification analysis of EGFP-PH$_{akt}$ and mRFP-FKBP-iSH2 upon $H_2O_2$ and FK506 stimulation, respectively. The PM/Cyto was calculated in the same way as in Figure 2c. The sharp spike in the upper trace is a single data point artefact from the addition of FK506.

50 nM FK506. Half-life ($t_{1/2}$) values for iSH2 domain release were significantly more sensitive to alterations of the FK506 concentration (Figure 2d). However, the observed differences appeared to have little effect on the rate of $PIP_3$ turnover suggesting that iSH2 release at higher FK506 concentrations (0.5 µM and above) does not significantly contribute to the change in $PIP_3$ levels. In fact, the apparent lack of PI3K activity enabled us to quantify PTEN activity levels by calculating the kinetic parameters $K_{cat}/K_m$ based on the single-cell traces (Figure S8). For this purpose, we estimated the $PIP_3$ concentration[17] and used the Schnell–Mendoza equation to extract the kinetic parameters from the decay curves of $PIP_3$.[18] Also, we determined the average number of PTEN molecules in HeLa cells by quantitative Western blotting[19] in order to calculate the $K_{cat}$ value. Importantly, the in vivo $K_{cat}$ values appear to be much higher than those for PTEN in vitro, listed in the BRENDA database (see Supporting Information).

To further confirm the role of PTEN in $PIP_3$ degradation, we blocked PTEN activity by adding $H_2O_2$, a procedure known to oxidize the catalytically active cysteine residues of PTEN (Figure 2e,f).[20] Subsequent FK506 addition immediately released the iSH2 domain from the plasma membrane but not the $PH_{Akt}$ domain. The translocation ratio of the $PH_{Akt}$ domain was slowly reverting, probably driven by slow recovery of PTEN activity or by catalysis through other much less active phosphatases. The plasma membrane staining by $PH_{Akt}$ was fully visible even after 5 min (Movie S4).

One of the prime functions of $PIP_3$ is the recruitment and activation of various Akt isoforms at the plasma membrane, which in turn leads to modulation of other downstream signaling components such as FoxO1 and p70S6 kinase in the PI3K/Akt/mTOR pathway (Figure 3a). We were therefore interested in comparing the drop in $PIP_3$ levels with the changes in phosphorylation levels of Akt and downstream signaling effectors on a minute timescale by Western blots. We showed that after addition of FK506, the released Akt was very quickly dephosphorylated at Ser473, indicating that the switch-off signal is transferred from the lipid to the protein level within a few minutes. In addition, we checked the phosphorylation levels of FoxO1 that is directly regulated by Akt and of p70S6 kinase that is activated by Akt through the mTOR pathway (Figure 3b). We found that FK506 addition reduced the phosphorylation levels of both enzymes over time. Comparison of the phosphorylation level of those three proteins (Figure 3c, Figure S5) revealed that Akt is dephosphorylated with the fastest kinetics, followed by FoxO1 and p70S6 kinase. This demonstrates that the metabolic switch off effect after $PIP_3$ breakdown decayed depending on the immediacy of the downstream proteins and the signal lipids within the signaling network. Our reversible dimerization system clearly provides a novel approach to dissect the dynamics of this and other complicated signaling networks.

In summary, we present a reversible chemical dimerizer translocation technique sufficiently fast and complete to quantify enzyme activity and/or the half-life of metabolites, here shown for turnover of a second messenger lipid in intact cells. We determined that the PTEN activity (Figure S8) is very high, in fact much higher than in vitro studies suggested so far and implying that a significant $PIP_3$ signal is only

  

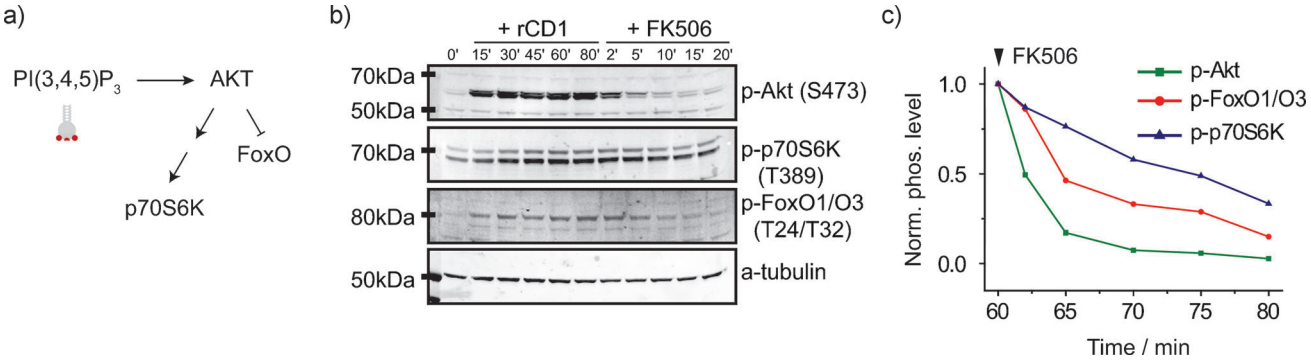


***Figure 3.*** Analysis of protein phosphorylation downstream of $PIP_3$. HeLa Kyoto cells transfected with Lck-ECFP-SNAP$_f$ and mRFP-FKBP-iSH2 were treated with rCD1 and followed after FK506 addition at different time points as indicated above. a) Simplified PI3K/Akt signaling pathway. b) Cell lysates were immunoblotted with different phosphoprotein antibodies as depicted. c) Changes of normalized phosphorylated protein levels after addition of FK506 over time (see Supporting Information for quantification details).

generated after PI3K activity overcomes that of PTEN. This in turn suggests that the complete machinery of $PIP_3$ biosynthesis and metabolism is generally very fast and relatively small changes in the equilibrium are able to induce or stop the $PIP_3$ driven signal. Due to the very rapid end of the $PIP_3$ signaling, we were able to perform a "relaxation-type" of experiment and follow the downstream signaling using standard biochemical techniques including the dephosphorylation of downstream signaling proteins. A similar effect could be induced by uncaging lipids such as $PIP_3$[21] or diacylglycerol.[22] However, contrary to the present experiments, we would not know if the signaling event had reached its maximal effectiveness.

The rCD1 is easily accessible in two steps from commercial reagents and the design of constructs for our technique is similar to the popular rapamycin system. In addition, the new quantification method that we developed (Figure S6) allows precise monitoring of the protein translocation from time-lapse image data. In general, the method will be suitable to measure many different metabolic processes in intact cells in the future.

Received: February 11, 2014
Published online: May 19, 2014

**Keywords:** FKBP · PI3K · $PIP_3$ · reversible chemical dimerizer · SNAP

[1] J. Chatterjee, M. Beullens, R. Sukackaite, J. Qian, B. Lesage, D. J. Hart, M. Bollen, M. Köhn, *Angew. Chem.* **2012**, *124*, 10200 – 10206; *Angew. Chem. Int. Ed.* **2012**, *51*, 10054 – 10059.
[2] a) M. Putyrski, C. Schultz, *FEBS Lett.* **2012**, *586*, 2097 – 2105; b) A. Rutkowska, C. Schultz, *Angew. Chem.* **2012**, *124*, 8288 – 8298; *Angew. Chem. Int. Ed.* **2012**, *51*, 8166 – 8176.
[3] P. Varnai, B. Thyagarajan, T. Rohacs, T. Balla, *J. Cell Biol.* **2006**, *175*, 377 – 382.
[4] B. C. Suh, T. Inoue, T. Meyer, B. Hille, *Science* **2006**, *314*, 1454 – 1457.
[5] T. Miyamoto, R. DeRose, A. Suarez, T. Ueno, M. Chen, T. P. Sun, M. J. Wolfgang, C. Mukherjee, D. J. Meyers, T. Inoue, *Nat. Chem. Biol.* **2012**, *8*, 465 – 470.
[6] F. S. Liang, W. Q. Ho, G. R. Crabtree, *Sci. Signaling* **2011**, *4*, rs2.
[7] M. Skwarczynska, M. Molzan, C. Ottmann, *Proc. Natl. Acad. Sci. USA* **2013**, *110*, E377 – 386.
[8] a) J. F. Amara, T. Clackson, V. M. Rivera, T. Guo, T. Keenan, S. Natesan, R. Pollock, W. Yang, N. L. Courage, D. A. Holt, M. Gilman, *Proc. Natl. Acad. Sci. USA* **1997**, *94*, 10618 – 10623; b) A. Keppler, S. Gendreizig, T. Gronemeyer, H. Pick, H. Vogel, K. Johnsson, *Nat. Biotechnol.* **2003**, *21*, 86 – 89; c) L. W. Miller, J. Sable, P. Goelet, M. P. Sheetz, V. W. Cornish, *Angew. Chem.* **2004**, *116*, 1704 – 1707; *Angew. Chem. Int. Ed.* **2004**, *43*, 1672 – 1675; d) S. Mizukami, S. Watanabe, Y. Hori, K. Kikuchi, *J. Am. Chem. Soc.* **2009**, *131*, 5016 – 5017; e) S. Watanabe, S. Mizukami, Y. Hori, K. Kikuchi, *Bioconjugate Chem.* **2010**, *21*, 2320 – 2326.
[9] D. Erhart, M. Zimmermann, O. Jacques, M. B. Wittwer, B. Ernst, E. Constable, M. Zvelebil, F. Beaufils, M. P. Wymann, *Chem. Biol.* **2013**, *20*, 549 – 557.
[10] Y. C. Lin, Y. Nihongaki, T. Y. Liu, S. Razavi, M. Sato, T. Inoue, *Angew. Chem.* **2013**, *125*, 6578 – 6582; *Angew. Chem. Int. Ed.* **2013**, *52*, 6450 – 6454.
[11] a) A. Levskaya, O. D. Weiner, W. A. Lim, C. A. Voigt, *Nature* **2009**, *461*, 997 – 1001; b) M. J. Kennedy, R. M. Hughes, L. A. Peteya, J. W. Schwartz, M. D. Ehlers, C. L. Tucker, *Nat. Methods* **2010**, *7*, 973 – 975; c) L. J. Bugaj, A. T. Choksi, C. K. Mesuda, R. S. Kane, D. V. Schaffer, *Nat. Methods* **2013**, *10*, 249 – 252; d) J. E. Toettcher, D. Gong, W. A. Lim, O. D. Weiner, *Nat. Methods* **2011**, *8*, 837 – 839.
[12] Y. I. Wu, D. Frey, O. I. Lungu, A. Jaehrig, I. Schlichting, B. Kuhlman, K. M. Hahn, *Nature* **2009**, *461*, 104 – 108.
[13] M. Baker, *Nat. Methods* **2012**, *9*, 443 – 447.
[14] P. A. Clemons, B. G. Gladstone, A. Seth, E. D. Chao, M. A. Foley, S. L. Schreiber, *Chem. Biol.* **2002**, *9*, 49 – 61.
[15] J. H. Bayle, J. S. Grimley, K. Stankunas, J. E. Gestwicki, T. J. Wandless, G. R. Crabtree, *Chem. Biol.* **2006**, *13*, 99 – 107.
[16] O. Idevall-Hagren, E. J. Dickson, B. Hille, D. K. Toomre, P. De Camilli, *Proc. Natl. Acad. Sci. USA* **2012**, *109*, E2316 – 2323.
[17] C. Y. Ung, H. Li, X. H. Ma, J. Jia, B. W. Li, B. C. Low, Y. Z. Chen, *FEBS Lett.* **2008**, *582*, 2283 – 2290.
[18] C. T. Goudar, J. R. Sonnad, R. G. Duggleby, *Biochim. Biophys. Acta Protein Struct. Mol. Enzymol.* **1999**, *1429*, 377 – 383.
[19] M. Schilling, T. Maiwald, S. Bohl, M. Kollmann, C. Kreutz, J. Timmer, U. Klingmüller, *FEBS J.* **2005**, *272*, 6400 – 6411.
[20] S. R. Lee, K. S. Yang, J. Kwon, C. Lee, W. Jeong, S. G. Rhee, *J. Biol. Chem.* **2002**, *277*, 20336 – 20342.
[21] M. Mentel, V. Laketa, D. Subramanian, H. Gillandt, C. Schultz, *Angew. Chem.* **2011**, *123*, 3895 – 3898; *Angew. Chem. Int. Ed.* **2011**, *50*, 3811 – 3814.
[22] A. Nadler, G. Reither, S. Feng, F. Stein, S. Reither, R. Müller, C. Schultz, *Angew. Chem.* **2013**, *125*, 6455 – 6459; *Angew. Chem. Int. Ed.* **2013**, *52*, 6330 – 6334.

  